Available online at www.sciencedirect.com

SciVerse ScienceDirect

Ceramics International 39 (2013) 1575–1581

CERAMICS INTERNATIONAL

www.elsevier.com/locate/ceramint

Ceramization and oxidation behaviors of silicone rubber ablative composite under oxyacetylene flame

Dong Yang, Wei Zhang*, Benzheng Jiang

College of Aerospace and Materials Engineering, National University of Defense Technology, Changsha 410073, China

Received 29 May 2012; received in revised form 31 July 2012; accepted 31 July 2012
Available online 15 August 2012

Abstract

Silicone rubber ablative composite filled with silica and carbon fibers was prepared and tested using an oxyacetylene torch. After the material was fired, the structure, composition and thermal-oxidative properties of the composite were analyzed. The results showed that a pyrolysis layer, a ceramic layer and a silica layer were formed in turn by decomposition, ceramization and oxidation reactions of the virgin ablative composite. Aromatic carbon was formed in the porous pyrolysis and ceramic layers by the degradation of the silicone rubber matrix, which transformed into inorganic carbon in the zone close to the silica layer. Crystallite growth of silicon carbide, the content of which is 10.2 wt% of the ablative products, is revealed in the ceramic layer. Oxidation of the compounds in the ceramic layer yields a silica layer, which is composed primarily of by silica. The thermo-oxidative stabilities of the ablative layers were better than that of the virgin material as a result of the formation of an inorganic ceramic structure.

Keywords: Silicone rubber composite; Ablation mechanism; Ceramization; Silicon carbide

1. Introduction

Silicone rubber based composite with silica (SiO_2) and carbon fibers is a promising ablative material for the thermal protection of solid rocket motor and ramjet combustor [1,2]. This composite has exceptional capability to withstand the fast-flowing, high temperature combustion gases and plays an important role in reducing the temperature rise of rocket motor cases. DC 93-104, a commercial silicone rubber ablative composite from Dow Corning Corporation, has endured many flight test successfully [3,4], which has set the stage for testing and reporting of numerous similar silicone rubber ablative composites [5–10].

In order to clarify the ablation mechanisms and establish ablation models for the present silicone rubber ablative composite, a detailed experimental study of the ablation process was initiated. Oyumi [11] suggested that after heating test, the silicone rubber ablative composite consisted of a virgin zone, a reaction zone and a char zone. Roberts and Chambers [12] reported that following heat ablation, the DC 93-104 was composed of five layers: virgin zone, volatilization zone, pyrolysis zone, transition zone and hard char zone. However, these researchers based their conclusions primarily on the morphologies of the ablated composite. Further work detailing the evolution of the ablated composite microstructure and the chemical transformation of the composite during ablation, particularly the transformation of the polymeric composite into the inorganic ceramic, has not yet been reported.

It is well known that a silicon carbide (SiC) ceramic can be produced by several methods, e.g., carbothermal reaction between SiO_2 and carbon by heat treatment or self-propagating high-temperature synthesis (SHS) [13], the reaction between carbon and molten silicon at high temperature [14,15], conversions from precursor to ceramic by heat treatment [16], polymer impregnation and pyrolysis (PIP) [17] and chemical vapor deposition (CVD) [18]. The oxidation of SiC has also been studied in details [19–21]. However, the ceramic formation and consumption process of polymeric composite under oxyacetylene flame has not been reported.

In this paper, a silicone rubber ablative composite filled with fumed SiO_2 and carbon fibers was prepared and then

*Corresponding author. Tel.: +86 731 84574785; fax: +86 731 84573183.
E-mail address: wzhang_nudt@nudt.edu.cn (W. Zhang).

0272-8842/$ - see front matter © 2012 Elsevier Ltd and Techna Group S.r.l. All rights reserved.
http://dx.doi.org/10.1016/j.ceramint.2012.07.109

tested using an oxyacetylene flame. Following firing, the microstructure and composition of the ablative composite were characterized. In addition, the thermal-oxidative properties of the ablated layers were investigated.

2. Experimental

2.1. Materials

Commercial Polydimethylsiloxane (PDMS) and polydimethylphenylsiloxane (PMPS) were produced by the Shanghai Resin Co., China. The average molecular weights were about 550,000 and 700,000, respectively. The vinyl contents of the two rubbers were both 0.15 mol%, the ratio of phenyl to methyl in PMPS was 1:10. Fumed SiO_2 (Degussa, Germany) with a BET surface area of 250 $m^2\,g^{-1}$ was used as a filler in the composites. We chose to use Toray's T300 (Toray Inc., Japan) carbon fibers as fillers for the composite. We also included 2,5-bis(tert-butylperoxy)-2,5-dimethylhexane, (Acros Organics Co., Belgium) a peroxide as a vulcanizator.

2.2. Composite preparation

Formula for the silicone rubber ablative composite is shown in Table 1.

The material was prepared in a two-roll laboratory model of an open mixing mill (length 600 mm × diameter 230 mm), the fibers were introduced as the last component to reduce the possibility of a breakdown of the fibers during mixing.

The refolded sheet was cut into cylinders with a thickness of 10 mm and a diameter of 30 mm, and then vulcanized in a mold at 433 K and 10 MPa for 15 min. The secondary vulcanization was carried out at 453 K for 2 h in an airflow drier.

2.3. Characterizations and measurements

A heat flux of 4152.9 $kW\,m^{-2}$ was created in the oxyacetylene flame test. The inner diameter of the flame nozzle was 2.0 mm. The distance between the specimen surface and the flame nozzle was 10 mm. After being burned for 20 s, the ablative properties of the sample were obtained by measuring its dimension and mass loss.

The equilibrium composition of oxyacetylene combustion products was calculated by the minimization-of-free-energy method. These results are shown in Table 2.

The microstructure of the ablative composite after ablation was characterized by a S4800 scanning electron microscopy (SEM, HITACHI). The elemental distribution of the ablative composite following ablation was studied using energy dispersive spectroscopy (EDS).

The crystal phases of the samples were identified by D8 ADVANCE X-ray diffraction (XRD, Bruker), utilizing Cu Kα radiation.

Fourier transform infrared (FTIR) spectra were obtained in the range 4000–400 cm^{-1} at a resolution of 1 cm^{-1} using a Nicolet FTIR spectrophotometer (AVATAR 360FT, USA) employing the KBr pellet technique.

Free carbon content was measured as the following procedure: the powdery sample of 2.0 g was placed in a crucible with the thickness less than 2.0 mm; after heating at 923 K for 1 h in a tube furnace under flowing oxygen atmosphere (400 mL min^{-1}), the free carbon content of the sample was determined according to the weight loss. SiO_2 content was determined using the following procedure: the powdery sample of 1.0 g was dissolved in 10 mL hydrofluoric acid using Teflon beaker as container, then the solution was vaporized in a sand bath at 473 K. The residue was then treated with 5 mL hydrofluoric acid in the same Teflon beaker and the solution was heated at 473 K until the sample was completely dry. The SiO_2 content of the sample was determined as being equal to the whole weight loss. The residual compound of the ablated material after the oxidation and hydrofluoric acid treatment was considered to be the SiC ceramic.

The thermal-oxidative properties of the samples were analyzed by thermogravimetric differential thermal analysis (Thermoflex, Rigaku Co., Japan) in air atmosphere heating the samples from room temperature to 1500 K, at heating rate of 20 K min^{-1}.

3. Results and discussion

3.1. Microstructure of the ablated composite

After the ablation by oxyacetylene flame, the dimension and mass loss of the silicone rubber ablative composite were determined. The linear and mass ablation rates of the ablative composite were only 0.0472 mm s^{-1} and 0.0605 g s^{-1}, respectively, indicating that the composite exhibits excellent anti-ablative properties.

Examination of the longitudinal profiles of the ablated composite (Fig. 1) revealed a multilayer ablation structure that can be divided into four parts. From the un-erosion material to the flame surface, these were virgin layer (Zone

Table 1
Formula of the silicone rubber ablative composite.

Ingredients	PDMS	PMPS	SiO_2	Carbon fiber	Peroxide
Contents (phr*)	50	50	30	15	1

*Parts per hundred grams of rubber (phr).

Table 2
Composition of the equilibrium combustion products.

Species	CO	CO_2	H	H_2	H_2O	O	OH	O_2
Fractions (mol%)	53.29	3.52	17.12	11.72	6.11	3.49	4.03	0.72

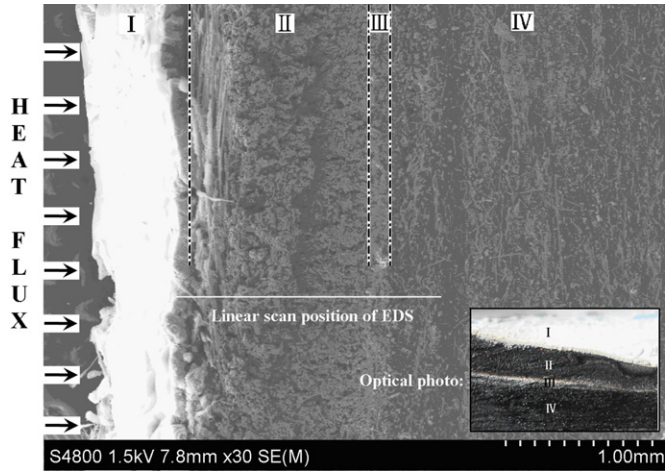

Fig. 1. Longitudinal profile image of the silicone rubber composite after ablation.

IV, black and dense), pyrolysis layer (Zone III, gray and porous), ceramic layer (Zone II, black and porous) and silica layer (Zone I, white and smooth). The pyrolysis layer was indistinguishable after the application of platinum coating on the sample prior to the SEM examination. The thickness of pyrolysis layer and silica layer were approximately 0.1 mm, while the thickness of ceramic layer was approximately 0.9 mm.

The cross sections of the four layers are shown in Fig. 2. Fig. 2a shows that silicone rubber and carbon fibers are well-combined in the virgin layer, but a loose structure is formed in the pyrolysis layer as shown in Fig. 2b, due to the degradation of silicone rubber [22]. The ceramic layer (Fig. 2c), which was transformed from pyrolysis layer at higher temperature, was more dense and rigid than the pyrolysis layer. This suggests that further reactions among the pyrolysis residues might be involved in the ceramization process. Oxidation of the ceramic layer took place in the oxyacetylene flame with oxidizing species (O_2, CO_2, O, OH and H_2O), then SiO_2 was likely produced to form the smooth silica layer (Fig. 2d).

3.2. Composition of the ablated composite

The position of the line profile of EDS is marked in Fig. 1, and the EDS results are shown in Fig. 3. The results showed that the maximum concentration of carbon, silicon and oxygen was in the Zone II (Ceramic layer), Zone IV (Virgin layer) and Zone I (Silica layer), respectively. The concentration of silicon decreased from the virgin layer to the middle of ceramic layer, due to the decomposition of silicone rubber. The high carbon content detected in the ceramic layer suggests that carbon may have been deposited in this zone from the pyrolysis products of the composite. Silicon and oxygen were predominately detected primarily in the silica layer (Zone I). Since the content of carbon of Zone I was approximately zero, this confirmed that SiO_2 was produced by oxidation reactions.

After ablation of the silicone rubber composite, the four individually identified layers (virgin layer, pyrolysis layer, ceramic layer and silica layer) were separated from each other and ground into powders for additional analysis. Because the silica layer was very thin and adhered firmly to the ceramic layer, when we peeled the silica layer from the ceramic layer, portions of the ceramic layer adhered to the silica layer which gave the silica layer a green tinge. Consequently, it is more accurate to describe this peeled layer as surface layer rather than silica layer.

The FTIR spectra of the virgin layer, pyrolysis layer, ceramic layer and surface layer are shown in Fig. 4. From virgin layer to surface layer, the FTIR peaks assigned to the vibrations of the methyl groups (–CH_3 deformation at 1412 cm^{-1}, C–H wagging at 1020 cm^{-1}, –CH_3 wagging at 1263 cm^{-1}, –CH_3 stretching at 2963 cm^{-1}) were gradually reduced or almost completely eliminated, indicating the scission of the organic structure in the silicone rubber. However, the FTIR peak at 1630 cm^{-1}, which is attributed to the stretching vibration of the benzene ring (C=C), became stronger in the spectra of pyrolysis and ceramic layers than that of virgin layer, suggesting some aromatic compounds (e.g., aromatic carbon) were formed in these two layers. In the FTIR spectra for the surface layer, there were only three main peaks associated with the stretching of Si–O (1097 cm^{-1} and 480 cm^{-1}) and Si–C (801 cm^{-1}) bonds, which indicated that the surface layer was composed primarily of SiO_2 and SiC, and most of the aromatic carbon has been eliminated. Therefore, these results indicate that the inorganic ceramic structure of the ablated composite was gradually created from virgin layer to surface layer.

Fig. 5 shows the XRD patterns of the ingredients (fumed SiO_2, silicone rubber and carbon fibers) of the composite. As shown in this figure, the 2θ values of the characteristic diffraction peaks for SiO_2, silicone rubber and carbon were 22.3°, 12.2° and 25.5°, respectively.

Fig. 6 shows the XRD patterns for the ablation layers of the silicone rubber composite. Some broad convexes were observed in the XRD patterns of these ablation layers, which indicated that the main substances in the ablated layers were amorphous. The XRD peak of silicone rubber ($2\theta = 12.2°$) became weak in the pyrolysis layer (Fig. 6b) and disappeared

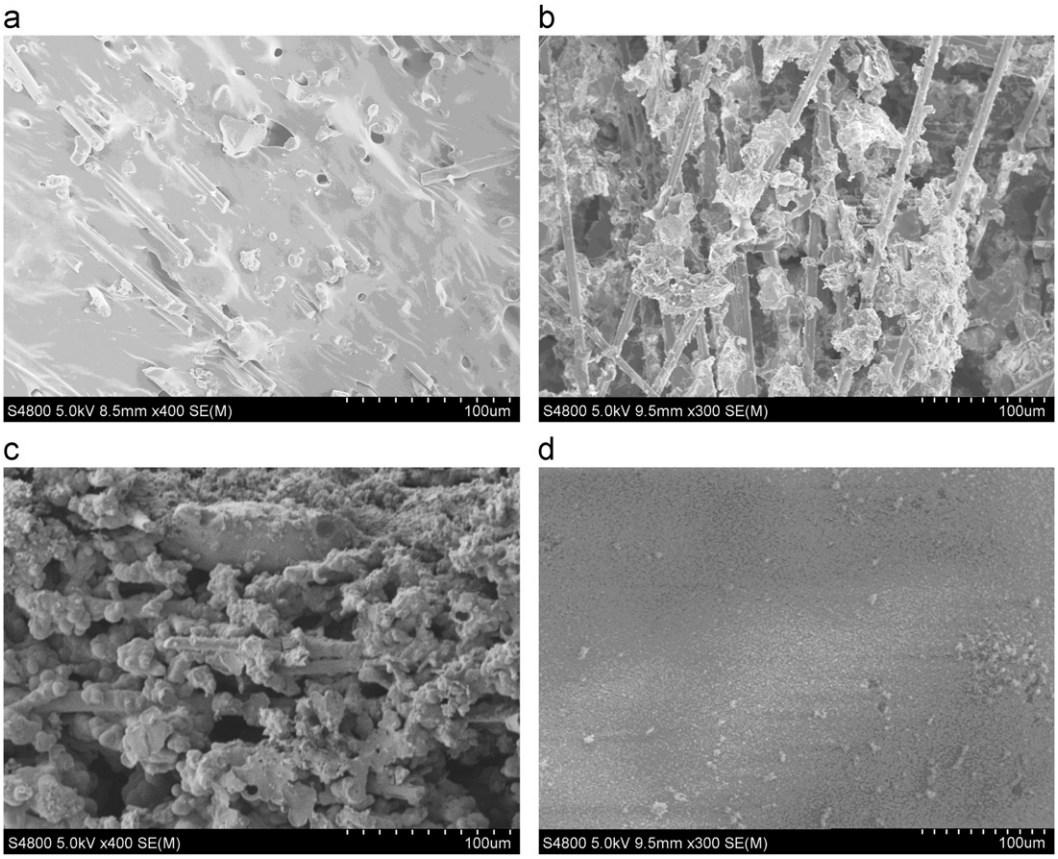

Fig. 2. SEM images for the cross section of the silicone rubber ablative composite after ablation (a) Virgin layer, (b) Pyrolysis layer, (c) Ceramic layer and (d) Silica layer.

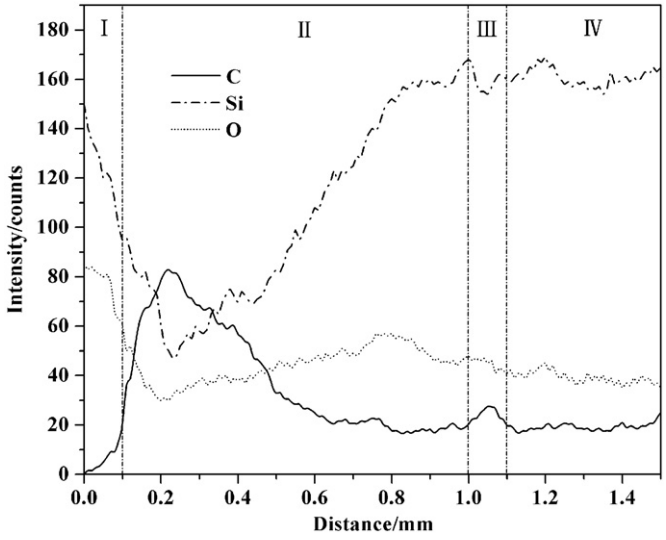

Fig. 3. Energy dispersive spectroscopy line profiles of carbon, silicon, and oxygen from ablation surface to the un-erosion zone.

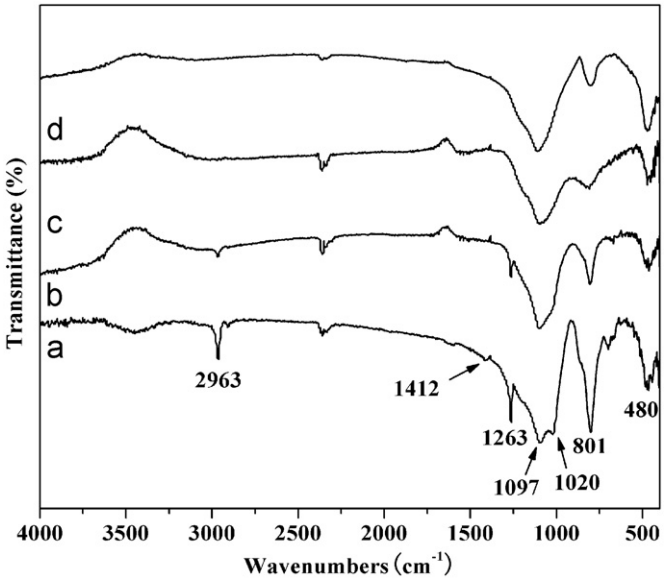

Fig. 4. FTIR spectra for (a) virgin layer, (b) pyrolysis layer, (c) ceramic layer and (d) surface layer of the silicone rubber ablative composite after ablation.

in the ceramic layer (Fig. 6c and d), suggesting the decomposition of silicone rubber with increasing temperatures. The hump around 2θ values of 25.5°, which is associated with the inorganic carbon, became more obvious in the ceramic layer (Fig. 6c and d) than in the virgin and pyrolysis layers (Fig. 6a and b). Part of the inorganic carbon is carbon fiber, and the other part may be derived from the aromatic carbon. In the XRD pattern of the surface layer (Fig. 6e), a strong broad

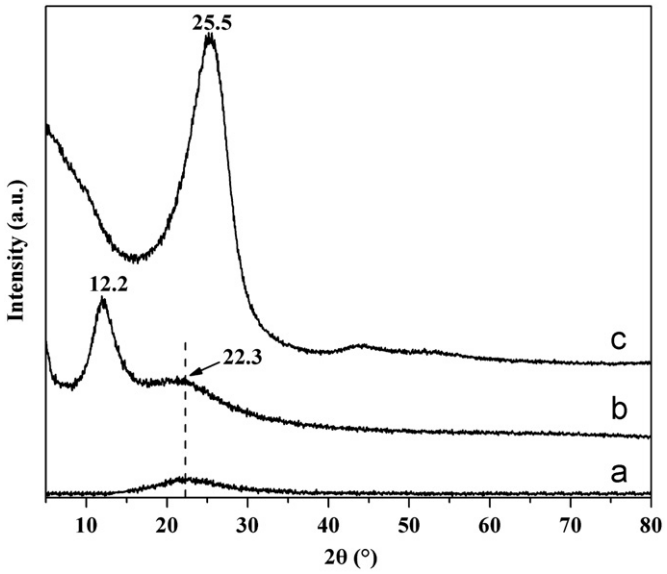

Fig. 5. XRD patterns of (a) fumed SiO_2, (b) SiO_2 filled silicon rubber and (c) carbon fibers.

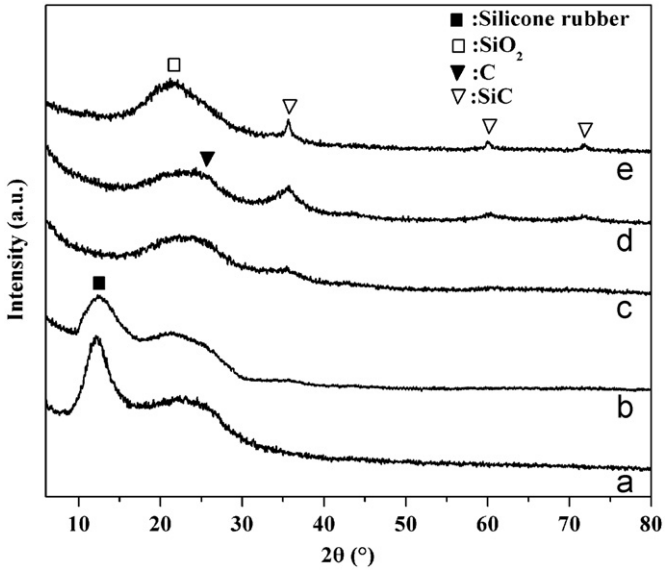

Fig. 6. XRD patterns of (a) virgin layer, (b) pyrolysis layer, (c) lower part of ceramic layer, (d) upper part of ceramic layer and (e) surface layer.

band of SiO_2 around 2θ of 22.3° predominated and the diffraction peak for carbon was not observed, suggesting that the carbon on the ablation surface was almost completely oxidized. The distribution of carbon in these ablation layers is consistent with the linear EDS results for the profile of the ablated composite (Fig. 3).

Additionally, three obvious diffraction peaks were present at about the 2θ values of 35.5°, 60.5° and 72.5° in the pattern of the upper part of ceramic layer (Fig. 4c) and surface layer (Fig. 4e), corresponding to the (111), (220) and (311) reflections of β-SiC. However, there was only a very weak peak at 2θ of 35.5° in the lower part of ceramic layer, suggesting the SiC content was quite low or in amorphous state in this zone. The XRD peaks for SiC of the surface layer were much narrower than those of the ceramic layer. The crystalline particle size d can be estimated from the breadth B of the diffraction peak at half-maximum [23]:

$$d = 0.94\lambda / B\cos\theta \quad (1)$$

where λ is the X-ray wave length and θ is the Bragg diffraction angle.

According to the XRD peak at 2θ value of 35.5° in Fig. 6c–e, B is about 3.00°, 2.21° and 0.49° in the lower part of ceramic layer, upper part of ceramic layer and surface layer, and the calculated crystallite size of SiC is 2.88 nm, 3.91 nm and 17.63 nm, respectively. It can be concluded from these results that SiC is in situ produced in the ceramic layer by siloxane ceramization or carbothermal reaction [24]. The crystallinity of SiC is not well developed in the lower part of the ceramic layer and the content of SiC phase may be also very low. In the upper ceramic layer at higher temperature, more SiC ceramic is produced and the amorphous SiC phase gradually transforms into crystalline state and yields crystalline particles with bigger size, especially in the zone close to the silica layer.

Table 3
Chemical composition of the ablative products of silicone rubber composite.

Species	Free carbon	SiO_2	In situ ceramic
Fractions (wt%)	21.8	68.0	10.2

Table 3 shows the composition of the ablative products (sum of silica, ceramic and pyrolysis layers) of the ablative composite measured by chemical analysis. SiO_2 was the main ingredient with the content of 68.0 wt%. The content of in situ SiC ceramic was 10.2 wt%. The rest was free carbon (21.8 wt%). Compared with the hydrocarbon rubber based ablative composites [25,26], whose char layers are exclusive carbon after ablation, the carbon content of the ablative products of silicone rubber based composite is relatively low.

Although SiO_2 shows excellent oxidation resistance, the melting point of SiO_2 (1986 K) is rather low, the blowing away of melted SiO_2 may occur in the ablation environment at high temperature. Because the SiO_2 content of the ablative products of silicone rubber composite is apparently excessive, the loss of melted SiO_2 is serious, and the increment of carbon and ceramic content may be beneficial to improve the ablation resistance of the composite.

3.3. Thermal oxidation of the ablated composite

The TG and DTA curves for the thermal-oxidative degradation of virgin layer, pyrolysis layer, ceramic layer and surface layer of the silicone rubber ablative composite following high temperature are presented in Figs. 7 and 8. The important characteristic data of TG curves are summarized in Table 4. The temperatures of 5% mass

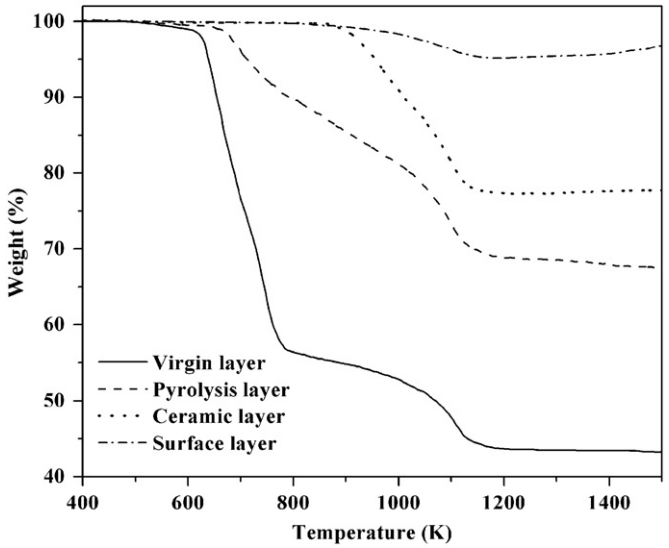

Fig. 7. TG curves for virgin layer, pyrolysis layer, ceramic layer and surface layer of the ablated composite.

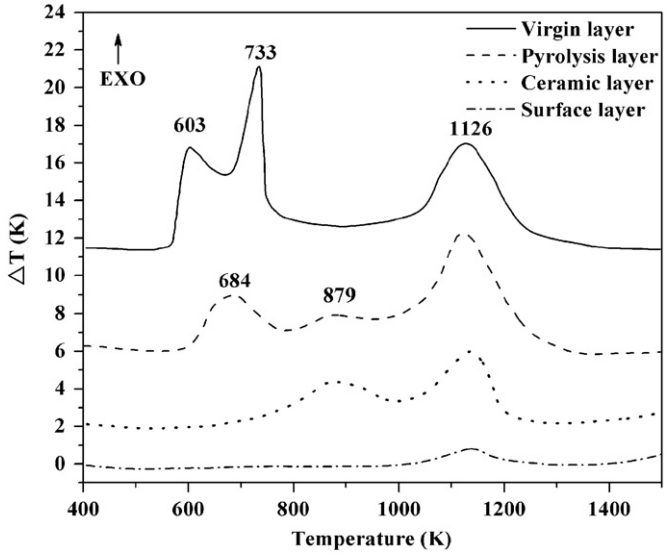

Fig. 8. TDA curves for virgin layer, pyrolysis layer, ceramic layer and surface layer of the ablated composite.

Table 4
TG results for virgin layer, pyrolysis layer, ceramic layer and surface layer in air atmosphere.

Sample	Temperature for 2% weight loss, T_{onset} (K)	Residual yield at 800 K (%)	Residual yield at 1200 K (%)	Residual yield at 1500 K (%)
Virgin layer	625	56.4	43.6	43.3
Pyrolysis layer	679	89.8	68.8	67.3
Ceramic layer	915	99.7	77.3	77.8
Surface layer	1019	99.8	95.2	96.8

loss (T_{onset}) for these ablation layers gradually increased from virgin layer (625 K) to surface layer (1019 K) by 394 K. It indicates that the initial thermal-oxidative stability of the samples is enhanced by the heat treatment of the oxyacetylene flame. At above 1200 K, the mass of all samples became almost stable, suggesting that the oxidation reactions which led to great weight loss (e.g. the oxidation of silicone rubber and carbon) were completed at 1200 K. The degradation residual weight at 1200 K also increased from 43.6% of virgin layer to 95.2% of surface layer. For the TG curves in the range of 1200–1500 K, the weight loss was gradual in virgin layer and pyrolysis layer, but a little weight increment was observed in the TG curves of ceramic layer and surface layer (Table 1), which was caused by the oxidation of SiC. These results suggest that the thermo-oxidative stability of the ablated composite is enhanced from virgin layer to surface layer.

Three degradation steps with strong exothermic signal were clearly observed in the thermal-oxidative process for the virgin layer of the composite in Figs. 7 and 8. The first degradation step around 603 K showed very little weight loss ($<3\%$). The greatest amount of weight loss ($\sim 42\%$) was detected in the second degradation step around 733 K. Overlapping of these above two DTA peaks was also observed. The first degradation step probably involves two oxidation reactions: a) peroxidation of the side groups of the silicone rubber with the oxygen in the air, which increases the weight of the rubber; b) deep oxidation of the organic side groups releasing small molecular weight gas (H_2O and CO_2), which leads to the weight loss of the rubber. The overlapping of the two oxidation reactions explains the small weight change but obvious exothermic character in the first oxidation step. It indicates that the second degradation step must be predominated by the deep oxidation of the organic side groups of the silicone rubber resulting in substantial weight loss and a strong exothermic signal. The third degradation step between 800 and 1200 K showed 11% weight loss and is associated with the oxidation of inorganic carbon (carbon fibers). It is well known that SiO_2 is stable below 1500 K, but carbon will be totally oxidized into CO_2 or CO at 1500 K in air. However, the residual weight (43.3%) of the composite at 1500 K was much greater than the content of SiO_2 (20.7%) in the silicone rubber composite. On the assumption that the oxidation residue at 1500 K is completely formed by SiO_2, it can be concluded that some silicon atoms ($\sim 33.7\%$) of the silicone rubber are oxidized into SiO_2, which may be one reason for the very high SiO_2 content in the ablative products by chemical analysis.

In the DTA curve of the pyrolysis layer of silicone rubber composite, the two peaks of peroxidation (603 K) and deep oxidation (733 K) of silicone rubber combines into one weak peak at 684 K. At the same time, the oxidation residual weight of pyrolysis layer (89.76%) was 33.4% higher than that of virgin layer (56.4%). This suggests that parts of organic groups in the silicone rubber are destroyed in the pyrolysis layer. The DTA peak for the

oxidation of carbon was still present between 800 and 1200 K. However, a new peak around 879 K was observed in the DTA curve of the pyrolysis layer, which might be assigned to the oxidation of aromatic carbon formed by the degradation of silicone rubber according to the FTIR results (Fig. 4).

The DTA peaks between 600 and 800 K disappeared in the DTA curve of the ceramic layer in air, suggesting the methyl groups of silicone rubber were totally cleaved in the ceramic layer. However, the DTA peaks for the oxidation of aromatic carbon and inorganic carbon were still observed. In other words, the relative content of carbon increased in the ceramic layer, which was consisted with the EDS results for the profile of the ablated silicone rubber composite (Fig. 3).

Only one weak DTA peak for the oxidation of inorganic carbon around 1126 K was observed in the DTA curve for the surface layer of the composite in air. It indicates that the aromatic carbon existing in the pyrolysis and ceramic layers may gradually transform into inorganic carbon near the silica layer at high temperature, followed by further oxidation of carbon occurs on the ablated surface under the oxyacetylene flame.

Following the DTA curves further shows that the ceramic layer and surface layer slowly exhibited exothermic reaction above 1300 K, suggesting the oxidation of SiC.

4. Conclusions

After ablation of the silicone rubber based ablative composite under the oxyacetylene flame, a pyrolysis layer, a ceramic layer and a silica layer were formed by decomposition, ceramization and oxidation reactions. With increasing temperature, the material transformed further into porous pyrolysis and ceramic layers containing aromatic carbon, due to the decomposition of silicone rubbers. In the ceramic layer, a zone with high carbon content was observed and SiC was also in situ produced. The crystallite size of SiC grew from 2.88 nm in the lower part of ceramic layer to 17.63 nm in the surface layer. A silica layer was formed by SiO_2, which was produced by the oxidation reaction of ceramic layer. The thermo-oxidative stabilities of these ablation layers were improved from virgin layer to surface layer by the formation of inorganic carbon, SiC and SiO_2.

References

[1] W.F. Vernon, F.E. Norman, Space Shuttle Solid Propellant Rocket Motors, Asbestos Filled Insulation Replacement, AIAA 1997-2992, 1997.

[2] Y. Susumu, S. Chouji, K. Kazushige, Thermal and Ablative Properties of Silicone Insulation, AIAA 1997-3259, 1997.

[3] J.A. Ramseyer, Elastomeric Composition Containing Silicon Carbide for use as an Ablative Coating, US Patent 3623904, 1971.

[4] F.F. Webster, Liquid Fueled Integral Rocket Ramjet Technology Review, AIAA 1978-1108, 1998.

[5] D.C. Sayles, Siloxane-based Elastomeric Inerceptor Motor Insulation, US Patent 4953476, 1990.

[6] H. Fujiki, M. Ohashi, H. Okamoto, Ablator Compositions, US Patent 5905101, 1999.

[7] G. Beall, Z. Shirin, S. Harris, M. Wooten, C. Smith, Development of an ablative insulation material for ramjet applications, Journal of Spacecraft and Rockets 41 (2004) 1068–1071.

[8] R. Sanden, Castable silicone based heat insulations for jet engines, Polymer Testing 21 (2002) 61–64.

[9] E.S. Kim, E.J. Kim, J.H. Shim, J.-S. Yoon, Thermal stability and ablation properties of silicone rubber composites, Journal of Applied Polymer Science 110 (2008) 1263–1270.

[10] E.S. Kim, T.H. Lee, S.H. Shin, J.-S. Yoon, Effect of incorporation of carbon fiber and silicon carbide powder into silicone rubber on the ablation and mechanical properties of the silicone rubber-based ablation material, Journal of Applied Polymer Science 120 (2011) 831–838.

[11] Y. Oyumi, Ablation characteristics of silicone insulation, Journal of Polymer Science Part A: Polymer Chemistry 36 (1998) 233–239.

[12] W.E. Roberts, J.W. Chambers, Investigation of silicone elastomers as ramburner insulators, in: ASME Intersociety Conference on Environmental Systems, San Diego, CA, 12–15 July, 1976, pp. 1–8.

[13] Z. Yermekova, Z. Mansurov, A. Mukasyan, Influence of precursor morphology on the microstructure of silicon carbide nanopowder produced by combustion syntheses, Ceramics International 36 (2010) 2297–2305.

[14] D. Mallick, O.P. Chakrabarti, H.S. Maiti, R. Majumdar, Si/SiC ceramics from wood of Indian dicotyledonous mango tree, Ceramics International 33 (2007) 1217–1222.

[15] Z. Yan, J. Liu, J. Zhang, T. Ma, Z. Li, Biomorphic silicon/silicon carbide ceramics from birch powder, Ceramics International 37 (2011) 725–730.

[16] Y. Ma, S. Wang, Z.-H. Chen, Raman spectroscopy studies of the high-temperature evolution of the free carbon phase in polycarbosilane derived SiC ceramics, Ceramics International 36 (2010) 2455–2459.

[17] W. Guo, H. Xiao, W. Xie, J. Hu, Q. Li, P. Gao, A new design for preparation of high performance recrystallized silicon carbide, Ceramics International 38 (2012) 2475–2481.

[18] Q.-G. Fu, H.-J. Li, X.-H. Shi, K.-Z. Li, J. Wei, Z.-B. Hu, Synthesis of silicon carbide nanowires by CVD without using a metallic catalyst, Materials Chemistry and Physics 100 (2006) 108–111.

[19] A. Maity, D. Kalita, N. Kayal, T. Goswami, O. Chakrabarti, P.G. Rao, Oxidation behavior of SiC ceramics synthesized from processed cellulosic bio-precursor, Ceramics International 38 (2012) 4701–4706.

[20] Y. Xiang, W. Li, S. Wang, Z.-H. Chen, Oxidation behavior of oxidation protective coatings for PIP-C/SiC composites at 1500 °C, Ceramics International 38 (2012) 9–13.

[21] Q.L. Jia, H.J. Zhang, S.P. Li, X.L. Jia, Effect of particle size on oxidation of silicon carbide powders, Ceramics International 33 (2007) 309–313.

[22] W.J. Zhou, H. Yang, X.Z. Guo, J.J. Lu, Thermal degradation behaviors of some branched and linear polysiloxanes, Polymer Degradation and Stability 91 (2006) 1471–1475.

[23] B.E. Warren, X-Ray Diffraction, Addison-Wesley, Reading MA, 1969.

[24] P. Colombo, Polymer-derived ceramics: 40 years of research and innovation in advanced ceramics, Journal of the American Ceramic Society 93 (2010) 1805–1837.

[25] Y. Guan, L.-X. Zhang, L.-Q. Zhang, Y.-L. Lu, Study on ablative properties and mechanisms of hydrogenated nitrile butadiene rubber (HNBR) composites containing different fillers, Polymer Degradation and Stability 96 (2011) 808–817.

[26] Y.Y. Jiang, X. Zhang, J.Y. He, L. Yu, R.J. Yang, Effect of polyphenylsilsesquioxane on the ablative and flame-retardation properties of ethylene propylene diene monomer (EPDM) composite, Polymer Degradation and Stability 96 (2011) 949–954.